www.cafetinnova.org

Indexed in
Scopus Compendex and Geobase Elsevier,
Geo-Ref Information Services-USA, List B of Scientific Journals, Poland, Directory of Research Journals

ISSN 0974-5904, Volume 09, No. 05

International Journal of Earth Sciences and Engineering

October 2016, P.P.1989-1998

Study on Mechanical Behaviors of Unsaturated Remolded Collapsed Loess

WANG KAI AND WANG LIANJUN
[1]*School of Civil Engineering, Beijing Jiaotong University, Beijing 100044, CHINA*
[2]*Beijing Key Laboratory of Track Engineering, Beijing 100044, CHINA*
Email: *11115318@bjtu.edu.cn; wangkaiacademic@126.com*

Abstract: A series of physical-mechanical tests and statistical analysis are conducted to investigate the mechanical behavior of unsaturated remolded collapsible loess, which includes deformation and strength behavior at different moisture capacity, degree of compaction, and confining pressure in order to assess stability of tunnel foundation base in loess. Results indicate that collapsible loess is easy to be compacted and the residual deformation potential can be controlled. At optimum moisture capacity of 14.5%,when the degree of compaction is not less than 0.95, the stress-strain curves of loess transform from strain softening to strain hardening as the confining stress increases, but the curves are always strain hardening when the compacting factor is 0.92,regardless of the change of the confining pressure. Increasing moisture capacity, confining pressure, or decreasing the degree of compaction will make the loess more strain hardening. There is a positive correlation between internal friction angle, cohesion and degree of compaction, contrary to the above, the correlation between those and moisture capacity is negative. Power-exponent function $y = A \cdot x^B$ can fit the relationship precisely. The concept of ultimate shear strength indexes, including ultimate internal friction angle ϕ_{m} and ultimate cohesion c_m, is established, and the statistical analysis indicates that as the moisture capacity increases, ϕ_{m} and c_m increases firstly and then decrease. The aforesaid relationship can be fitted precisely with Gaussian function $\phi_{\mathrm{m}}(c_m)=a \cdot exp(-((\omega-b)/c)^2)$. Based on the concept and relationship above, an easy and fast method, involving only moisture capacity, is provided to judge if the strength can meet the design requirement, and verify the suitability through field experiment.

Keywords: *Collapsed loess, Strength, Deformation, Degree of compaction, Moisture capacity, Ultimate internal friction angle, Ultimate cohesion, Tunnel foundation base*

1. Introduction

Collapsed loess is widely distributed in China especially Shanxi, Shaanxi, Gansu province. Along with the rapid development of railway construction in northwestern China, the research on strength and deformation behavior of loess has increasingly become a hot research field. In recent years, scholars conduct a series of correlative studies, and get lots of achievements, most of which merely establishes function relation of one variable ignoring coupling relationship between the shear strength function of moisture capacity and the dry density function of moisture capacity. Based on the aforementioned coupling relationship, this paper establish easy and intuitive formula to expound the function relationship between ultimate shear strength indexes (ultimate internal friction angle and ultimate cohesion) and moisture capacity, in order to provide references for strength theoretic research of unsaturated collapsible loess and field fast construction.

In view of uneven settlement, collapse, natural bridge, sink hole and other engineering defects, which occur in railway tunnel foundation base in loess area such as Zhengzhou-Xi'an passenger special line, this paper analyses collapsed loess located in the foundation base of Liutiaoshan tunnel at Dazhun-Shenchi railway. A series of compaction tests and triaxial tests were carried out to establish the functional relationship between shear strength indexes and each parameter, such as compacting factor, moisture capacity and confining pressure. Based on the coupling relationship between the shear strength function of moisture capacity and the dry density function of moisture capacity, come up with the concepts of ultimate strength index (including: ultimate internal friction angle, ultimate cohesion).Then by using the method of curve fitting, the function relationship between the aforementioned indexes and the moisture capacity can be obtained. In addition, an evaluation methodology, which can be used to assess the strength of tunnel foundation base, is come forward. And then verify the validity of this evaluation methodology by comparing the test values of cohesion and internal friction angle with the calculated values.

2. Basic test features

2.1. Physical property

The undisturbed soil sample, which is derived from foundation base of Liutiaoshan tunnel entrance whose mileage post is DK95+190～DK95+400, presents pale yellow and has porosity and homogeneity. The physical mechanics test revealed that this undisturbed loess belongs to low liquid limit clay according to "Code for design on subgrade of railway" and "Code for design of railway tunnel". Parameter values are given in Table 1.

Table 1: *Physical and mechanics parameters of undisturbed*loess

	Physical properties						
Soil site	**Specific gravity**	**Void ratio**	**Cohesion/kPa**	**Internal friction angle/°**	**Plastic limit/%**	**Liquid limit/%**	**Plasticity index**
DK95+190	15.5	0.919	10.7	25.3	15.7	24	8.3
DK95+300	16.2	0.916	10.5	25.2	16.9	26	9.1
DK95+390	15.9	0.917	10.6	25.4	15.2	23	7.8

2.2. Compaction behaviors

The moisture capacity of remolded loess sample used in compaction test contain8%, 10% 12%, 14%, 16%, 18%, 20% and 22%. Extra moisture capacity of 13%, 14.5%, and 15% were inserted according to the test result above. During the process of experiment, the soil sample didn't loosen, spill, and peel, and water didn't overflows, no matter the moisture capacity is high and low. From the above we can come to the conclusion that collapsible loess is easy to be compacted.

Dry density at different moisture capacity of collapsible loess is given in Figure 1.

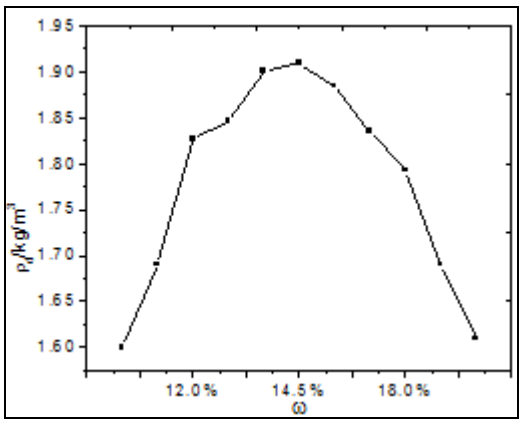

Figure 1: *Compaction curve of collapsible loess*

Figure 1 shows the changes in dry density of loess sample that occur at moisture capacity of 8%～22% in the compaction tests. The maximum dry density is $1.91\mathrm{g/cm^3}$ ($\rho_{\mathrm{dmax}}=1.91\mathrm{g/cm^3}$), and corresponding optimum moisture content is 14.5% ($\omega_{\mathrm{opt}}=14.5\%$), which is slightly less than its plastic limit. The compaction curve approximates saturation curve, which indicates that loess sample has high saturation and small void ratio at a dry density of $1.91g/cm^3$ (maximum dry density). In addition, the compaction curve on both sides of optimum moisture content is quite steep and asymmetrical. At the optimum moisture capacity, the air volume rate of loess sample of 5% is closer to clay, which indicates that when compactness of loess subgrade reaches 100%, its pore is almost filled, and residual plastic deformation can be effectively controlled under the force superstructure gravity and heavy haul train load.

3. Behavior of deformation and strength

As the most common failure mode of collapsible loess, the shear failure was simulated by means of triaxial compression test using TSZ-1 automatic triaxial apparatus. In order to investigate mechanics behavior of collapsible loess foundation at different confining pressure, different moisture capacity, and different degree of compaction, the moisture capacity of 8.5%～20.5% and the compacting factor of 0.81～0.98 were taken into consideration respectively in the UU triaxial tests, in view of concrete features of the project. Firstly, prepare loess sample at optimum moisture capacity, and then compound different moisture capacity sample with back pressure saturation method and humidifying method etc. And the different degree of compaction can be realized by controlling dry density of a soil sample. In addition to these elements above, effect of confining pressure on mechanics behavior of loess was analyzed by setting four different confining pressure of $50kPa$, $100kPa$, $200kPa$, and $500kPa$ for each group test. As a result the number of the sample is approximately 184.

3.1. Deformation behavior

Figure 2a-d show deformation behavior curve of loess sample at optimum moisture capacity of 14.5%, under different confining pressure and different degree of compaction.

There is a gradual increase in yield strength as the compacting factor increases from 0.92 to 0.97,and the strain softening behavior becomes more pronounced as the compacting factor increases.

The confining pressure affects the stress-strain relation significantly as well. For loess samples at a compacting factor of 0.97, as confining pressure is 50kPa and 100kPa, there is an obvious peak strength on the stress strain curve (typical softening behavior), and the failure mode is brittle failure. As confining

pressure is 200kPa and 500kPa, the failure mode turns to plastic failure, and there is no obvious peak strength on the stress-strain curve (typical hardening behavior). For loess sample with compacting degree of 0.95, only at a confining pressure of 500kPa, the peak strength appeared on the stress-strain curve, and as confining pressure increases, the failure mode turns into plastic failure from brittle failure. For compacting factor of 0.92 and 0.93, there is no obvious peak strength and the plastic failure always occurs whatever confining pressure is.

Analyses indicate that unsaturated collapsible loess has poor plasticity and it is more readily to appear brittle failure at a low confining pressure level. And as confining pressure increased from 50kPa to 500kPa, strain-hardening behavior becomes more marked, and the loess is more prone to have plastic failure. In addition, the unsaturated collapsible loess of high compacting degree has a certain degree of dilatancy.

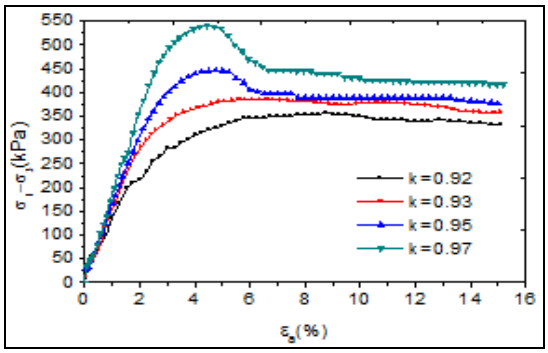

(a)*Confining pressure of 50kPa*

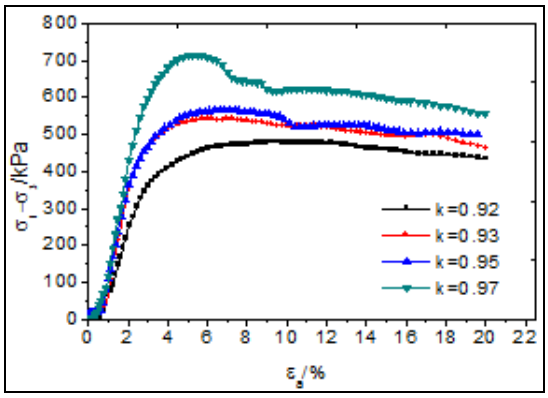

(b)*Confining pressure of 100kPa*

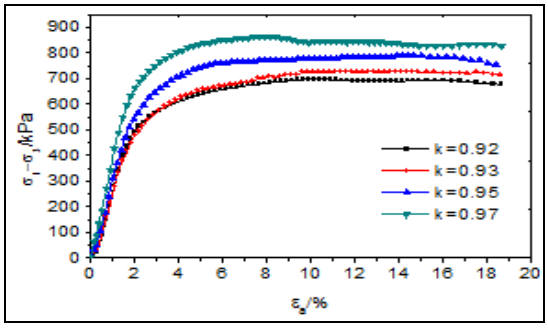

(c)*Confining pressure of 200kPa*

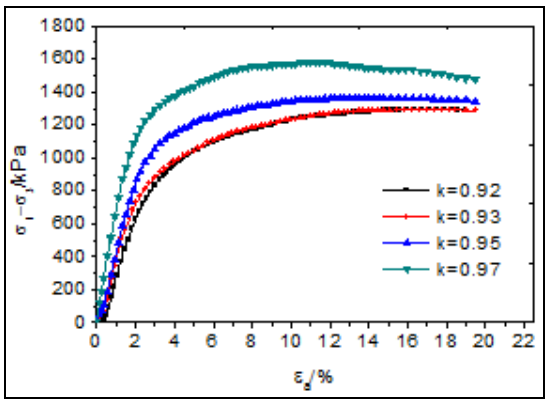

(d)*Confining pressure of 500kPa*

Figure 2: *Deformation behavior for loess with different compaction factor at optimum moisture capacity*

Figure 3a-d, 4a-d, and5a-d show the deformation behavior of loess samples at different moisture capacity. As the moisture capacity increased from 12.5% to 16.5%, the yield strength reduced gradually, initial stiffness decreased as well, and the strain hardening behavior became more significant. The analysis indicates that there is a decrease in the strength and modulus of compressibility as the moisture capacity increases.

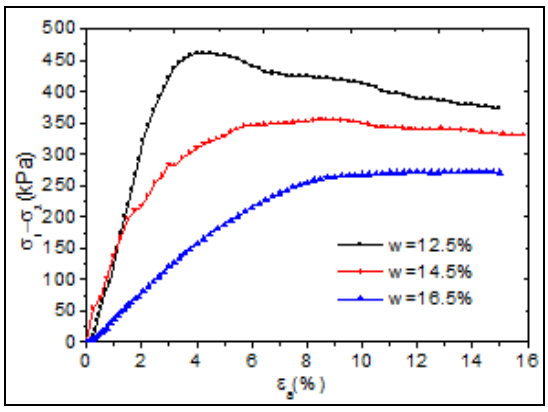

(a)*Compaction factor of 0.92, confining pressure of 50kPa*

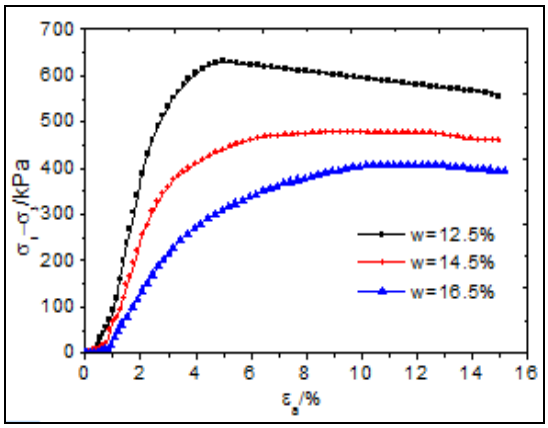

(b)*Compaction factor of 0.92, confining pressure of 100kPa*

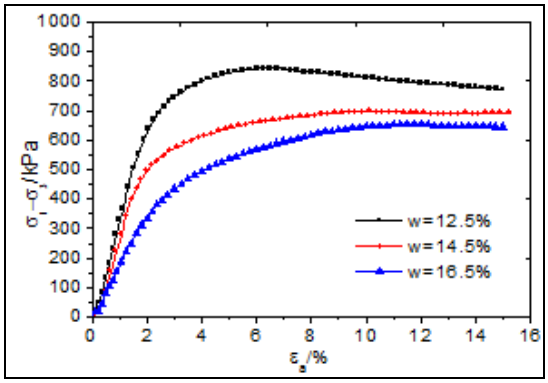

(c)Compaction factor of 0.92, confining pressure of 200kPa

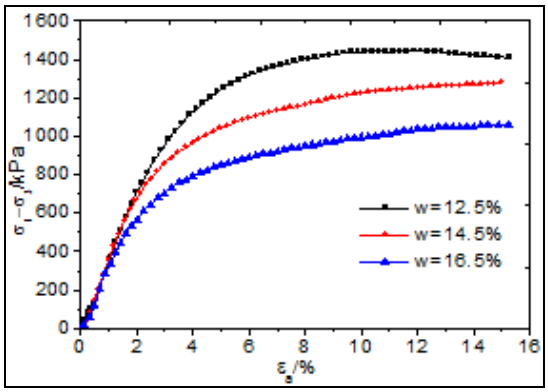

(d)Compaction factor of 0.92, confining pressure of 500kPa

Figure 3: *Stress-strain curve of loess at compaction factor of 0.92*

Figure 3a-d show the stress-strain curve of loess sample at compaction factor of 0.92. For the sample at confining pressure of 50kPa and 100kPa, the stress-strain curve is strain softening when the moisture capacity is 12.5%, and as the moisture capacity increases, the deformation behavior of loess sample transforms to hardening from softening gradually, which indicates the failure type changes from brittle failure to ductile failure. For the sample at confining pressure of 200kPa and 500kPa, the curves of any moisture capacity are strain hardening.

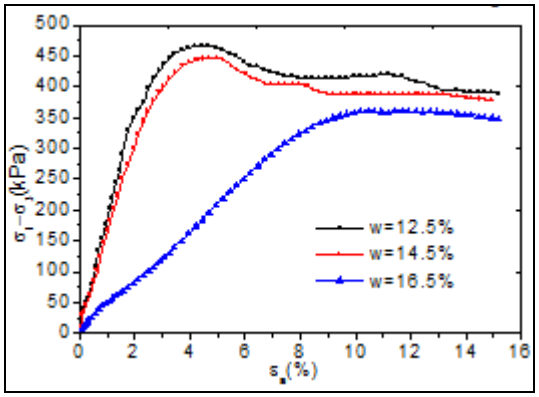

(a) *Compaction factor of 0.95, confining pressure of 50kPa*

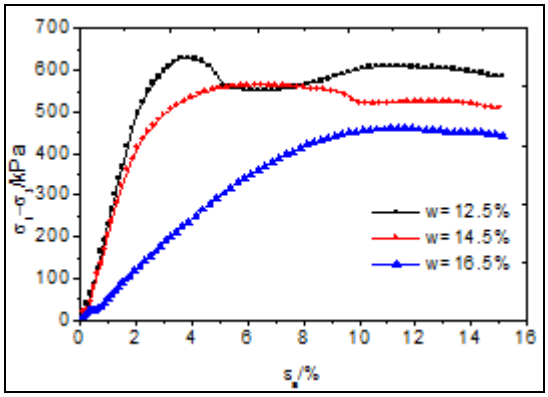

(b)*Compaction factor of 0.95, confining pressure of 100kPa*

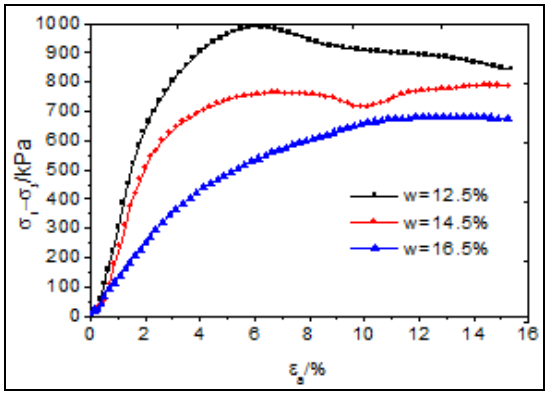

(c)*Compaction factor of 0.95, confining pressure of 200kPa*

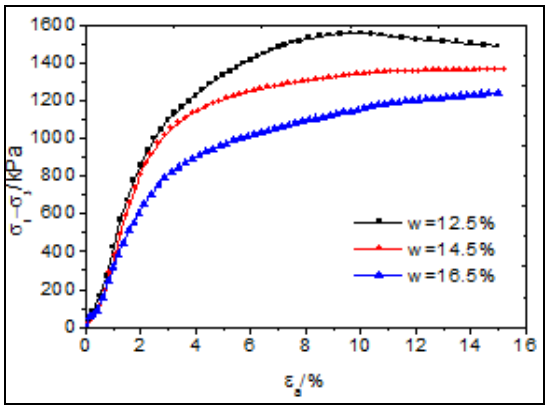

(d)*Compaction factor of 0.95, confining pressure of 500kPa*

Figure 4: *Stress-strain curve of loess at compaction factor of 0.95*

Figure4a-d show the stress-strain curve of loess sample at compaction factor of 0.95. For the sample at a confining pressure of 50kPa, when the moisture capacity is 12.5% and 14.5%, the stress-strain curve is strain softening. But at confining pressure of 100kPa, and 200kPa, the stress-strain curve is strain softening only when the moisture capacity is 12.5%.And for the above loess sample, as the moisture capacity increases, the deformation behavior of loess sample transforms to hardening from softening gradually. The

curves of loess at confining pressure of 500kPa are hardening at any moisture capacity.

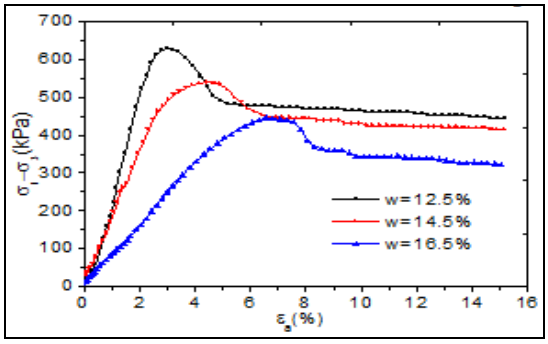

(a)Compaction factor of 0.97, confining pressure of 50kPa

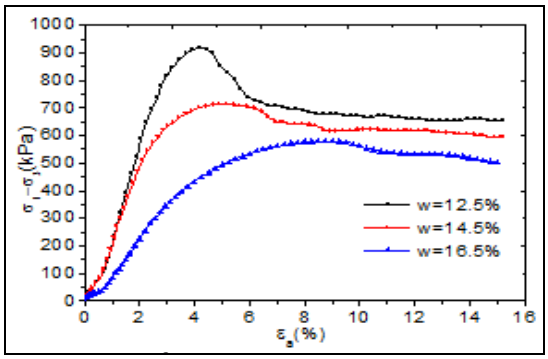

(b)Compaction factor of 0.97, confining pressure of 100kPa

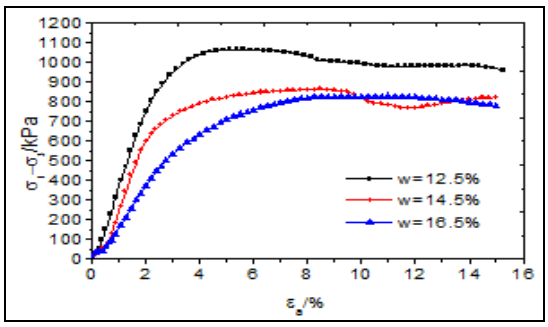

(c)Compaction factor of 0.97, confining pressure of 200kPa

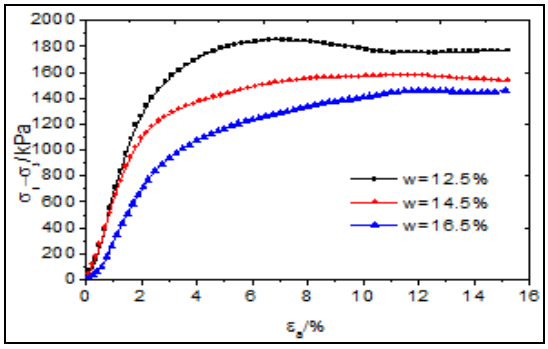

(d)Compaction factor of 0.97, confining pressure of 500kPa

***Figure 5:** Stress-strain curve of loess at compaction factor of 0.97*

Figure 5a-d show the stress-strain curves of loess samples at compaction factor of 0.97. For the sample at a confining pressure of 50kPa, all the curves are strain softening, but for the sample at 100kPa, only the curves of 12.5% and 14.5% are softening. But at confining pressure of 200kPa and 500kPa, the curves of any moisture capacity are hardening. What's more, as the moisture capacity increases, the deformation behavior of loess sample transforms to hardening from softening gradually.

3.2. Strength behavior

Calculate the shear strength (internal friction angle ϕ and cohesion c), and plot the relation curve (Figure 6) of ϕ, c and ω, k. Analyze the functional relationship between ϕ, c and ω, k through curve fitting. Parameters values are given in Table 2 and 3. Conclusions are as follows: 1) Under the same moisture capacity, there is a positive correlation between ϕ, c and k respectively, and as degree of compaction k increases from 0.92 to 0.97, the internal friction angle ϕ increases slightly 9°, but the cohesion c increases significantly 90kPa; 2)Under the same degree of compacting, there is a negative correlation between ϕ, c and ω respectively. As the moisture capacity ω increases from 12.5% to 16.5%, the internal friction angle ϕ slightly decreases 9°, but the cohesion c decreases 120kPa significantly. So the cooperation effect of internal friction angle ϕ and cohesion c leads the shear strength to reduce under humidification; 3) At the optimum moisture capacity, the maximum dry density can be attained through compacting, but the shear strength isn't maximum as with the internal friction angle ϕ and cohesion c; 4) The function relationship between ϕ, c and ω, k can be fitted with logarithmic function (Formula 1,2,3,and 4) accurately. The parameters are given in Table 2 and 3.

$$\phi = A_1 \cdot k^{B_1} \quad (1)$$

$$c = A_2 \cdot k^{B_2} \quad (2)$$

$$\phi = A_3 \cdot \omega^{B_3} \quad (3)$$

$$c = A_4 \cdot \omega^{B_4} \quad (4)$$

Where A_1 A_2 A_3 B_1 B_2 and B_3 are parameters.

Figure 6 and Table 2 and 3 show that as the moisture capacity keeps constant, there is a gradual increase in ϕ and c as the degree of compacting increases. It is known that under a constant moisture capacity, as the compacting energy increases, the dry density

increases. Hence, when the field compacting energy, used in construction, is less than that used in the laboratory compaction test, there is a maximum degree of compaction in construction under a certain moisture capacity. As result, under a certain moisture capacity, there is a maximum cohesion (defined as ultimate cohesion c_m) and a maximum internal friction angle (defined as ultimate internal friction angle ϕ_m) in foundation construction accordingly.

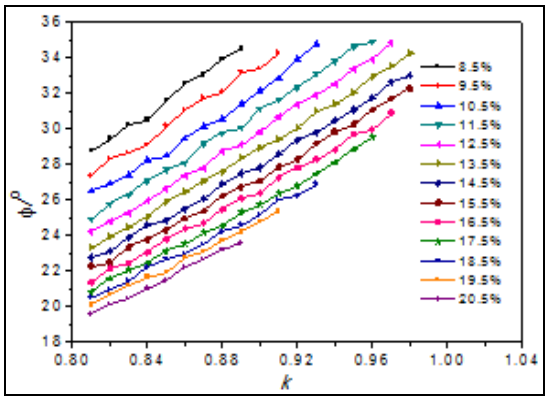

(a)*Relation curve between* ϕ *and* k

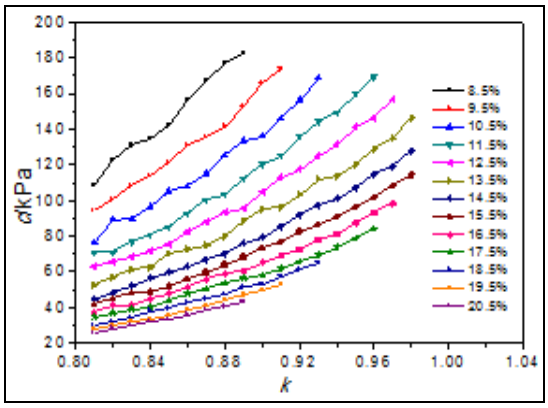

(b)*Relation curve between* c *and* k

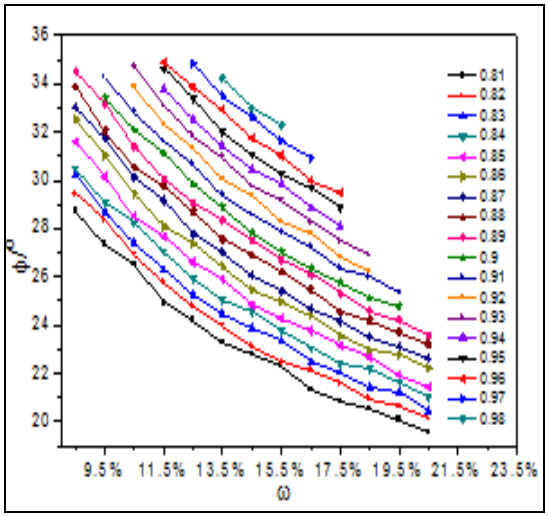

(c) *Relation curve between* ϕ *and* ω

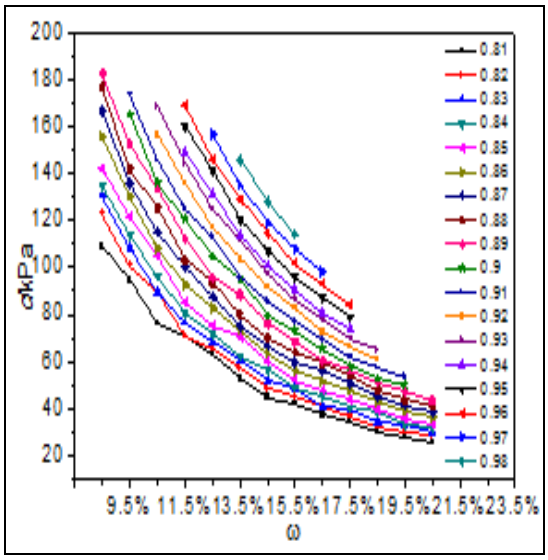

(d) *Relation curve between* c *and* ω

Figure 6: *Relation curves of shear strength and moisture capacity, compaction factor*

Table 2: *Parameters of the shear strength functions of the compaction factor under different moisture capacity*

ω	Parameters					
	A_1	B_1	R-square	A_2	B_2	R-square
8.5%	43.52	1.975	0.9937	345.5	5.331	0.9872
9.5%	41.14	0.920	0.9917	281.5	5.181	0.9958
10.5%	39.71	1.981	0.9938	244.9	5.341	0.9925
11.5%	38.17	1.990	0.9976	211.3	5.437	0.9975
12.5%	36.94	2.017	0.9990	183.2	5.295	0.9976
13.5%	35.64	2.000	0.9992	159.8	5.241	0.9962
14.5%	34.44	1.978	0.9987	141.8	5.394	0.9989
15.5%	33.59	1.984	0.9986	126.9	5.334	0.9989
16.5%	32.74	1.997	0.9981	114.8	5.342	0.9978
17.5%	31.84	1.995	0.9986	102.7	5.200	0.9970
18.5%	31.00	1.963	0.9971	95.82	5.452	0.9975
19.5%	30.47	1.969	0.9976	89.22	5.531	0.9968
20.5%	29.93	2.018	0.9952	80.59	5.349	0.9970

Table 3: *Parameters of the shear strength functions of the moisture capacity under different compaction factor*

k	Parameters					
	A_3	B_3	**R-square**	A_4	B_4	**R-square**
0.81	9.771	-0.4373	0.9973	2.019	-1.625	0.9950
0.82	10.01	-0.4379	0.9978	1.924	-1.686	0.9975
0.83	10.32	-0.4336	0.9982	2.035	-1.686	0.9989
0.84	10.83	-0.4212	0.9980	2.25	-1.662	0.9993
0.85	10.85	-0.4326	0.9984	2.461	-1.652	0.9972
0.86	11.08	-0.4349	0.9977	2.534	-1.671	0.9993
0.87	11.26	-0.4375	0.9988	2.663	-1.675	0.9992
0.88	11.76	-0.4271	0.9983	2.85	-1.670	0.9980
0.89	11.95	-0.4302	0.9985	3.231	-1.639	0.9988
0.9	12.18	-0.4300	0.9981	3.206	-1.673	0.9977
0.91	12.72	-0.4207	0.9989	3.484	-1.660	0.9991
0.92	12.29	-0.4488	0.9977	3.567	-1.680	0.9995
0.93	12.62	-0.4471	0.9982	3.603	-1.707	0.9995
0.94	13.26	-0.4315	0.9979	3.884	-1.689	0.9992
0.95	13.55	-0.4323	0.9958	4.024	-1.704	0.9978
0.96	14.34	-0.4124	0.9958	4.607	-1.665	0.9996
0.97	14.27	-0.4279	0.9975	4.467	-1.707	0.9957
0.98	14.32	-0.4346	0.9805	4.095	-1.784	0.9996

Curve fit the functional relationship of moisture capacity and dry density, and find that Fourier function (Formula 2) is the best fitting function (only applied to the moisture capacity span from 8% to 22%), and the correlation coefficient R^2 is 0.9762. The fitting curve is given in Figure 7.

$$\rho_d = a_0 + a_1 \cdot \cos(c \cdot \omega) + b_1 \cdot \sin(c \cdot \omega) \quad (2)$$

Where ρ_d is dry density, a_0 a_1 b_1 c are coefficients, which are given in Table 4.

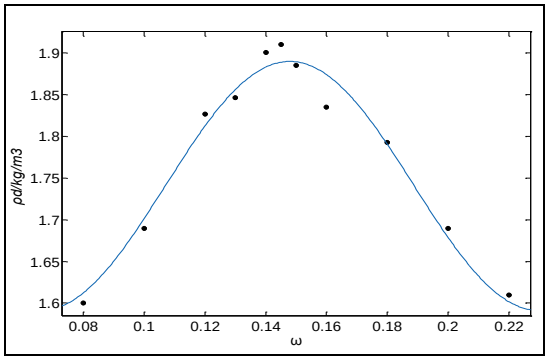

Figure7: *Fitting curve of moisture capacity and dry density*

Table 4: *Coefficients of relationship between moisture capacity and dry density*

Coefficients	**Values**
a_0	1.74100
a_1	0.12270
b_1	-0.08515
c	38.38000

According to Formula 2, calculate the ultimate compaction factor k_m at a certain moisture capacity. The values are given in Table5.

Table 5: *Ultimate compaction factor at different moisture capacity*

ω	ρ_d **/kg/m^3**	k_m
10.5%	1.7297	0.9056
11.5%	1.7863	0.9352
12.5%	1.8363	0.9614
13.5%	1.8724	0.9803
14.5%	1.9100	1.0000
15.5%	1.8848	0.9868
16.5%	1.8593	0.9735
17.5%	1.8166	0.9511
18.5%	1.7629	0.923
19.5%	1.7060	0.8932
20.5%	1.6542	0.8661

Plug the ultimate compaction factor k_m in Table 5 into corresponding equations in Table 2 and 3, then the ϕ_m and c_m under a certain moisture capacity can be calculated. ϕ_m and c_m values are given in Table 6.

Table 6: *Ultimate internal friction angle and ultimate cohesion at different moisture capacity*

ω	ϕ_m /°	c_m **/ kPa**
10.5%	32.6280	144.2069
11.5%	33.4058	146.7936
12.5%	34.1204	148.7314
13.5%	34.2400	143.9757
14.5%	34.4400	141.8000
15.5%	32.7160	118.2170

16.5%	31.0303	99.4564
17.5%	28.8094	79.1310
18.5%	26.4882	61.9064
19.5%	24.3944	47.7705
20.5%	22.3933	37.3536

Curve fit the data in Table 6withGaussion equation, and the result indicates that the data relativity between ϕ_m, c_m and ω is good. The fitting equations are given in Formula 3 and 4, and the fitting curves are shown in Figure8a-b.

$$\phi_m = a_1 \cdot exp(-((\omega - b_1)/c_1)^2) \quad (3)$$

$$c_m = a_2 \cdot exp(-((\omega - b_2)/c_2)^2) \quad (4)$$

Where $a_1\ b_1\ c_1\ a_2\ b_2\ c_2$ are parameters which are shown in Table 7.

Table 7: *Parameters of relationship between* ϕ_m, c_m *and* ω

Parameters	Value
a_1	34.3
b_1	0.1303
c_1	0.1114
a_2	150.9
b_2	0.1217
c_2	0.06812

The analysis indicates that as the moisture capacity increases, the ultimate internal friction angle ϕ_m and ultimate cohesion c_m increase firstly and reach a maximum when the moisture capacity is 13%, and then reducewith the increase of confining pressure.The moisture capacity where the maximum of ϕ_m and c_m occur is less than the optimum moisture capacity.

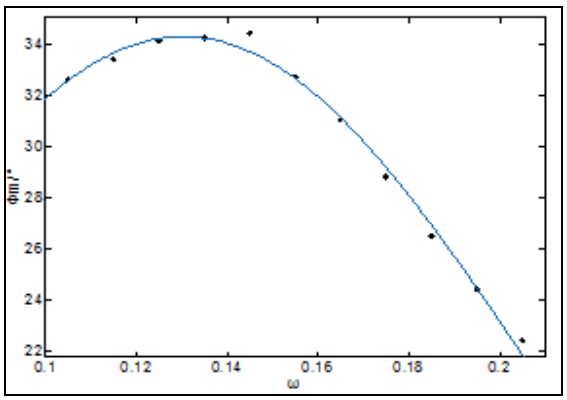

(a)*Relation curve of* ϕ_m *and* ω

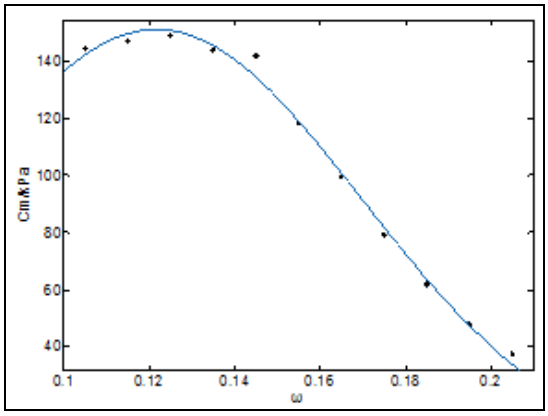

(b)*Relation curve of* c_m *and* ω

Figure 8: *Fitting curve of ultimate internal friction angle, ultimate cohesion and moisture capacity*

4. Engineering Application

In order to remove the collapsibility of loess, reduce the collapsible deformation, and enhance the bearing capacity, the loess foundation is stabilized with the method of composite foundation, dynamic compaction, and rolling.

For undisturbed collapsible loess, it's a remolded process to construct lime-soil compaction pile. Changing moisture capacity and compaction degree of loess between piles has the functions in two aspects: Firstly, the loess soil structure is damaged through compacting, leading to a loss of loess structural strength before railway operation. Secondly, the cohesion and internal friction angle are altered affecting the shear strength of loess. There is a direct effect of shear deformation and shear strength on the bearing capacity of tunnel subgrade buried in collapsible loess. Therefore, in order to obtainthe better quality of composite foundation, the moisture capacity and compaction degree of loess between piles should be strictly controlled.

In addition, only when the ultimate internal friction angle and ultimate cohesion of loess between piles under a certain moisture capacity are more than designed strength index, the tunnel foundation has a chance to meet the design requirement. If not, there is no possibility to offer enough bearing capacity. So this study puts forward the concepts of ultimate cohesion and ultimate internal friction angle, and investigates the functional relationship between them and moisture capacity to provide theory basis for easy and fast evaluation methodology involving only moisture capacity ("MCE" for short). The method can be used to evaluate the result of composite foundation construction of loess between piles. Definitely, this method applies to other loess treatment.

Test sections of a collapsible loess foundation in Dazhun-Shenchi heavy haul railway are reinforced with the method of rolling, dynamic compaction, and lime-soil compaction pile. Each method exerted

592kJ/ m^3 respectively in accordance with standard proctor compaction test according to "Specification of soil test" SL237-1999. Set different moisture capacity ranging from 12.5% to 16.5% for test sections foundation, and measure the degree of compaction, cohesion and internal friction angle after construction.

In order to verify the validity of this evaluation methodology, compare the test values of cohesion and internal friction angle with the calculated values. Choose two test sites to analyze, and the field measured and calculated data is compared in Table 8 and 9.

Table 8: *Comparison between calculated strength and those measured after dynamic compaction*

ω		**12.5%**	**13.5%**	**14.5%**	**15.5%**	**16.5%**
Measure data	k	0.9620	0.9810	0.9980	0.9890	0.9750
	ϕ /°	34.0911	34.2303	34.5012	32.7010	30.960
	c /kPa	147.6943	142.8896	142.6933	117.3160	98.5443
Calculated data	k	0.9614	0.9803	1.0000	0.9868	0.9735
	ϕ_m /°	34.1204	34.2400	34.4400	32.7160	31.0303
	c_m /kPa	148.7314	143.9757	141.8000	118.2170	99.4564

Table 9: *Comparison between calculated strength and those measured after lime-soil compaction pile*

ω		**12.5%**	**13.5%**	**14.5%**	**15.5%**	**16.5%**
Measure data	k	0.9625	0.9813	0.9989	0.9889	0.9756
	ϕ /°	34.1123	34.2298	34.4967	32.6978	30.8932
	c /kPa	146.9978	142.9880	143.1350	116. 6130	97.9893
Calculated data	k	0.9614	0.9803	1.0000	0.9868	0.9735
	ϕ_m /°	34.1204	34.2400	34.4400	32.7160	31.0303
	c_m /kPa	148.7314	143.9757	141.8000	118.2170	99.4564

Check the calculated parameters against the field measured strength parameters, as a result, the maximum difference of k , ϕ and c is 0.223%, 0.442%, and 1.475%. There is generally close agreement between the calculated strength in this paper and those measured in test sites, hence the MCE method can apply to engineering practice of loess foundation treatment in heavy haul railway.

5. Conclusions

Based on the compaction test, triaxial test and mathematical analysis above, the major conclusions can be summarized as follows.

(1) The compaction curve on both sides of optimum moisture content shows quite steep and asymmetrically, indicating the collapsible loess is sensitive to moisture content. The loess with the maximum dry density has high saturation degree and low void ratio. Thus when the degree of compaction of subgrade is pretty high, its pore is almost filled, and the residual plastic deformation under the force superstructure gravity and heavy haul train load can be effectively controlled.

(2) For samples withthe optimum moisture, when the degree of compaction is not less than 0.95, the stress strain curve transforms from strain softening to strain hardening gradually as the confining pressure increases from 50kPa to 500kPa. When the degree of compaction is 0.92, the curve is always strain hardening. The strain hardening phenomenon shows more obvious for samples with higher confining pressure, lower compaction degree or higher moisture content.

(3) Moisture content and degree of compaction have considerable effect on strength behavior of unsaturated collapsible loess. The strength as well as the initial rigidity reduces gradually with the increase of the moisture content. A power-exponent function $y = A \cdot x^B$ can be adopted to fit precisely the relationship between internal friction angle, cohesion and moisture content, degree of compaction respectively. Both the internal friction angle and cohesion exhibit positive correlativity with the degree of compaction and negative correlativity with the moisture content.

(4) The concept of ultimate shear strength index, including ultimate internal friction angle ϕ_m and ultimate cohesion c_m, is put forward. Both ϕ_m and c_m increase firstly and then decrease with the moisture, reaching the maximum value when the moisture capacity is 13%, which is less than the optimum moisture content. The correlativity can be fitted precisely by applying Gaussionfunction $\phi_m(c_m)=a \cdot exp(-((\omega-b)/c)^2)$.

(5) A method to judge the strength of loess subgrade is proposed, with only one parameter, moisture content, to be determined. The difference

between the field test results and calculated data by this method is less than 2%.

6. Acknowledgements

The work described in this paper is carried out under the auspices of Beijing Key Laboratory of Track Engineering. The authors are grateful to SN ENGR. Mao and Ir. Lee for offering information about Liutiaoshan tunnel at Zhun-Chi heavy haul railway. As well, the authors are grateful to Dr. D. Venkat Reddy, Prof. Liu Chuanzheng and Prof. Zhou Shunhua for providing the constructive comments.

References

[1] CHEN Zhenghan, "On basic theories of unsaturated soils and special soils", *Chinese Journal of Geotechnical Engineering*, Vol. 36, No. 2, pp. 201-272, 2014.

[2] K. Yuan, "The Formula Study of Strength Index for Remolded Loess", *International Conference on Mechatronics, Electronic, Industrial and Control Engineering (MEIC)-2015*, pp. 666-669, 2015.

[3] Z. Wang, "Study of undisturbed loess stress-strain experiments based on CT", *5th International Conference on Advanced Design and Manufacturing Engineering (ICADME)-2015*, pp. 2031-2038, 2015.

[4] Z. Zhong, Y. Liu, X. Liu, X. Li, and S. Wang, "Influence of moisture content on shearing strength of unsaturated undisturbed quaternary system middle pleistocene", *JOURNAL OF CENTRAL SOUTH UNIVERSITY*, Vol. 22, No. 7, pp. 2776-2782, 2015.

[5] X. Xing, T. Li and Y. Fu, "Determination of the related strength parameters of unsaturated loess with conventional triaxial test", *ENVIRONMENTAL EARTH SCIENCES*, Vol. 75, No. 821, 2016.

[6] J. Lipiec, M. Turski, M. Hajnos, and R. Swieboda, "Pore structure, stability and water repellency of earthworm casts and natural aggregates in loess soil", *GEODERMA*, Nol. 243, pp. 124-129, 2015.

[7] GUAN Liang, CHEN Zhenghan, HUANG Xuefeng, SUN Shuguo, FANG Xiangwei,"STUDY OF WETTING DEFORMATION OF UNSATURATED REMOLDEDLOESS", *Chinese Journal of Rock Mechanics and Engineering*, Vol. 30, No. 8, pp 1698–1704, 2011.

[8] FANG Xiangwei, CHEN Zhenghan, SHEN Chunni, WANG Hewen, LIU Houjian,"TRIAXIAL SHEAR PROPERTIES OF UNDISTURBED LOESS Q2",*Chinese Journal of Rock Mechanics and Engineering*, Vol. 27, No. 2, pp 383–389,2008.

[9] CHEN Zhenghan,"Deformation, strength, yield and moisture changeof a remolded unsaturated loess", *Chinese Journal of Geotechnical Engineering*, Vol. 21, No. 1, pp 82–90, 1999.

[10] LI Yongle, ZHANG Hongfen, SHI Xiaoguang, HOU Jinkai, YANG Lile,"Experimental study of triaxial test of undisturbed unsaturated loess", *Rock and Soil Mechanics*, Vol. 29, No. 10,pp 2859–2863,2008.

[11] LIAO Hongjian, LI Tao, PENG Jianbing,"Study of strength characteristics of high and steep slope landslide mass loess", *Rock and Soil Mechanics*, Vol. 32, No. 7, pp 1939–1944,2011.

[12] ZHANG Maohua, XIE Yongli, LIU Baojian,"Analysis of shear strength characteristics ofloess during moistening process", *Rock and Soil Mechanics*, Vol. 27, No. 7, pp 1195–2000,2006.

[13] FENG Zhiyan, QIU Bensheng, X IE Dingyi, "Experimental study of triaxial test of loess",*J.Xi'an Univ .of Arch .& Tech .(Natural Science Edition)*,Vol. 42, No.6,pp 803–808,2010.

[14] Yang Youhai, Wang Liqin, Su Zaichao, CHAI Zhancong,"The Study about Intensity Characteristic and Influence Factors of Remolded Loess", *JOURNAL OF LANZHOU RAI LWAY UNIVE RS ITY (Natural Sciences)*,Vol. 22, No. 3, pp 38–41,2003.

[15] XIAO Junhu, LIU Jiankun, PENG Liyun, CHEN Lihong,"Effects of compactness and water Yellow-River alluvialsilt content on its mechanical behaviors", *Rock and Soil Mechanics*, Vol. 29, No.2, pp 409–414,2008.

[16] LI Shibo, WANG Changming, MA Jianquan, WANG Gangcheng,"Microscopic changes of Longxi loess during triaxial shear process", *Rock and Soil Mechanics*, Vol. 34, No.11,pp 3299–3305,2013.

[17] CHEN Cunli, ZHANG Dengfei, DONG Yuzhu, CHEN Hui, YU Dianbo, XUE Junxiu,"Suction and mechanical behaviours of unsaturated intact loess from constant water content triaxial tests", *Chinese Journal of Geotechnical Engineering*, Vol. 36, No. 7,pp 1195–1202, 2014.

[18] Feng Yongyang, "Subgrade reinforcement for Collapsible Loess of Dazhun-Shenchi Heavy Haul railway", *RAILWAY CONSTRUCTION TECHNOLOGY*, No. 10, pp. 53–55,2013.

[19] China Railway Eryuan Engineering Group CO.LTD. TB 10106—2010Technical code for ground treatment of Railway Engineering. Beijing: China Railway Publishing House,2010.

[20] Nanjing Hydraulic Research Institute. SL 237—1999Specification of soil test. Beijing: China Water & Power Press,1999.